Pinning and Dynamics of Colloids on One Dimensional Periodic Potentials

C. Reichhardt and C.J. Olson Reichhardt
Center for Nonlinear Studies and Theoretical Division, Los Alamos National Laboratory, Los Alamos, New Mexico 87545
(February 2, 2008)

Using numerical simulations we study the pinning and dynamics of interacting colloids on periodic one-dimensional substrates. As a function of colloid density, temperature, and substrate strength, we find a variety of pinned and dynamic states including pinned smectic, pinned buckled, two-phase flow, and moving partially ordered structures. We show that for increasing colloid density, peaks in the depinning threshold occur at commensurate states. The scaling of the pinning threshold versus substrate strength changes when the colloids undergo a transition from one-dimensional chains to a buckled configuration.

PACS numbers: 82.70.Dd

Assemblies of interacting colloidal particles in two dimensions (2D) have attracted considerable attention as an ideal model system in which various types of equilibrium phases and melting transitions can be studied conveniently [1]. Some attractive features of this system include the fact that the colloid-colloid interactions and density can be changed easily and that the individual colloid positions and motions are directly accessible. Further, when a 1D or 2D periodic substrate is added to the system, unique ordering and melting transitions appear. In experiments on colloids interacting with 1D substrates created using interfering laser beams, a novel laser induced freezing was observed in which the colloids freeze into a crystal as the substrate strength is increased [2]. This substrate-induced freezing effect has also been studied theoretically [3] and numerically [4]. At even higher substrate strengths, a reentrant laser induced *melting* can occur when the laser or substrate strength is large enough that the colloids behave one-dimensionally and the fluctuations are effectively enhanced, as predicted initially in theoretical studies [4]. In this case, the colloids form a smectic state. Laser induced freezing and melting have subsequently been studied both experimentally [5] and theoretically [6,8]. A rich variety of other equilibrium phases for varied colloid density on 1D substrates have been predicted [8] and in some cases experimentally confirmed [9]. More recently the crystalline phases and melting of colloids interacting with 2D periodic substrates have been studied and a variety of novel crystalline orderings and melting phenomena were shown to occur [10–13].

Far less is known about the *dynamical* interactions of colloids with periodic substrates. Recently it was shown that dynamical locking effects can occur for colloids driven over 2D periodic substrates when the colloids preferentially move along the symmetry directions of the substrate [14–16]. These locking effects may be potentially useful as a technique for separating particle mixtures. Colloids driven over periodic substrates are also a useful model system for studying depinning phenomena. Similar systems in which depinning on periodic substrates occurs include vortices in superconductors interacting with 1D and 2D periodic pinning arrays [17] as well as models for atomic friction [18].

In this work we consider colloids driven over periodic 1D substrates, which to our knowledge has not been studied previously. We consider parameters relevant to recent experiments on colloids interacting with periodic potentials. For fixed substrate strength and lattice constant, we find that as the density of the colloids increases, peaks in the depinning threshold occur at various commensurate fillings. In general we observe a pinned regime, a disordered or plastic flow regime, and partially ordered moving regimes as a function of driving force. Several types of pinned states appear, include pinned commensurate lattices, pinned smectics, and buckled pinned configurations. For high colloidal densities where the colloids form a smectic state, we show that as the substrate strength decreases there is a change in the scaling of the depinning force versus substrate strength when the colloids undergo a transition from 1D chains to a buckled state.

We simulate a two-dimensional system of N_c colloids with periodic boundary conditions in the x and y-directions. The overdamped equation of motion for colloid i is

$$\frac{d\mathbf{r}_i}{dt} = \mathbf{f}^i_{cc} + \mathbf{f}_s + \mathbf{f}_d + \mathbf{f}_T \tag{1}$$

Here the colloid-colloid interaction force is $\mathbf{f}^i_{cc} = -\sum_{j\neq i}^{N_c} \nabla_i V(r_{ij})$, where we use a Yukawa or screened Coulomb potential given by $V(r_{ij}) = (q_i q_j/|\mathbf{r}_i - \mathbf{r}_j|)\exp(-\kappa|\mathbf{r}_i - \mathbf{r}_j|)$. $q_{i(j)} = 1$ is the colloid charge, $1/\kappa$ is the screening length, and $\mathbf{r}_{i(j)}$ is the position of particle $i(j)$. The substrate is periodic in 1D as shown in Fig. 1(a), with period d in the y-direction, $\mathbf{f}_s = f_p \sin{(2\pi y/d)}\hat{\mathbf{y}}$. This is the form expected from the modulated laser fields used in the experiments [5].

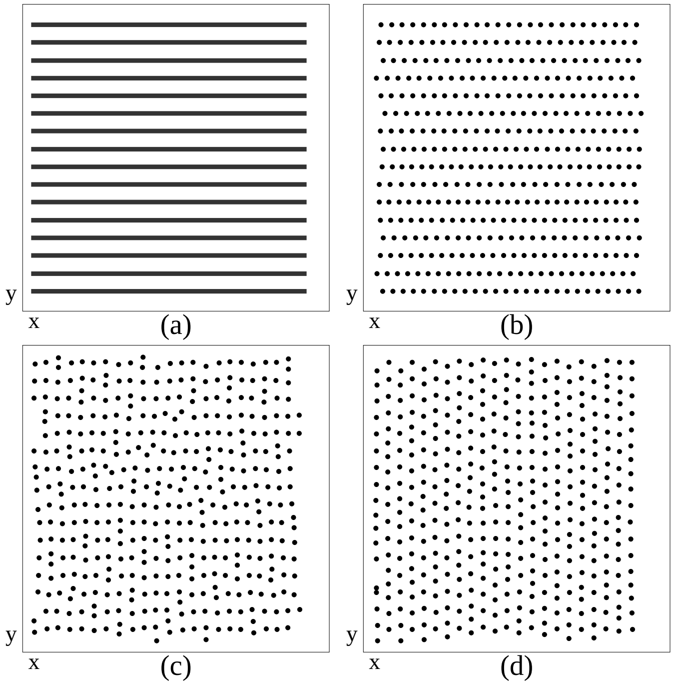

FIG. 1. (a) Heavy lines indicate the locations of the substrate minima. (b-d) Colloid configurations (black dots) for a system with fixed d, fixed $f_p = 2.0$, and $n_c = 1.35$. (b) $f_d = 0.0$ where a pinned smectic state occurs. (c) $f_d/f_c = 1.1$, where f_c is the depinning threshold. The colloids are moving in the y direction. (d) $f_d/f_c = 1.2$. Here the colloids show significant triangular ordering.

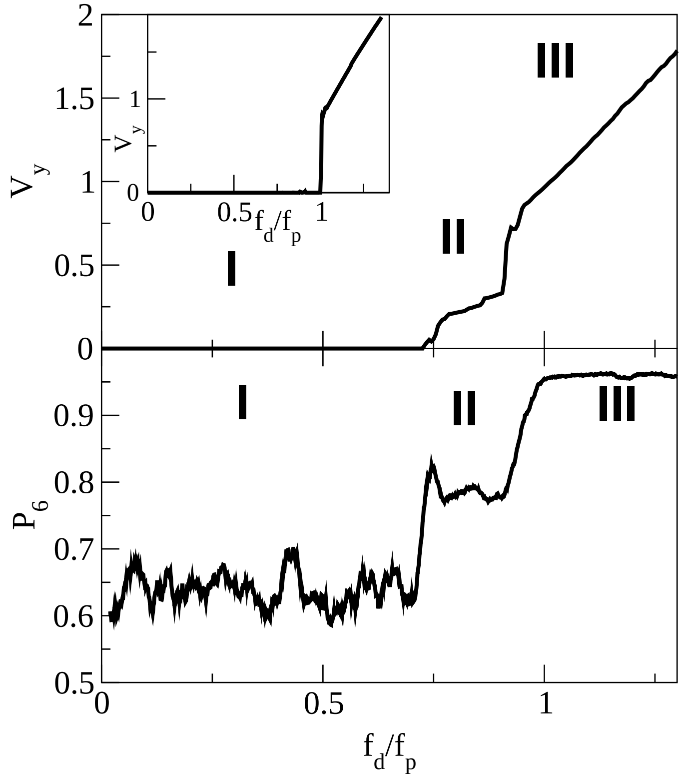

FIG. 2. (a) Average colloidal velocity V_y vs f_d/f_p for the system in Fig. 1 with $f_p = 2$ and $n_c = 1.35$. Inset: V_y vs f_d/f_p for $n_c = 0.375$. (b) The density of six-fold coordinated colloids P_6 vs f_d/f_p for the system in Fig. 1.

The external driving force is $\mathbf{f}_d = f_d\hat{\mathbf{y}}$ which could come from an applied electric field. The thermal force $\mathbf{f}_T$ is a randomly fluctuating force from Langevin kicks. We measure lengths in units of d, the substrate periodicity. We have considered various system sizes; here we focus on fixed $L_y = 16d$. A triangular colloidal lattice is commensurate with the substrate for $d = \sqrt{3}a/2$, where a is the colloidal lattice constant. The density of colloids, n_c, is normalized such that at the commensurate density, $n_c = 1.0$. Temperature is reported in terms of the melting transition temperature T_m for a colloidal lattice at the commensurate density in the absence of the substrate. For the results in this work we focus on the case $T/T_m = 0.5$ which is low enough to avoid appreciable creep. The initial colloidal state is obtained at zero external drive by cooling the system from a high temperature molten state to a lower temperature. A similar procedure was used to find the equilibrium states for colloids on 2D substrates [10]. The applied drive is then increased from $f_d = 0.0$ by small increments. At each increment, we measure the average colloidal velocity $V_y = \sum_{i=1}^{N_c} \mathbf{v}_i \cdot \hat{y}$ after reaching the steady flow state.

We first consider the case of fixed substrate lattice constant d and strength f_p and examine the depinning as a function of colloidal density n_c. In general we find three regimes: pinned, disordered flow, and a partially ordered high drive flow. The exact type of order in the pinned regime depends on the colloid density. For high densities $n_c > 1.0$, the colloids form a pinned smectic state, as seen in Fig. 1(b) for $n_c = 1.35$. At most densities, including this one, the colloid lattice is not commensurate with the substrate, so the potential minima capture differing numbers of particles and there are dislocations present in the lattice with Burgers vectors aligned parallel to the substrate. These dislocations depin before the particles do as the drive is increased so the colloids generally initially depin into a plastic flow regime or two phase flow regime where only a portion of the colloids move. In Fig. 1(c) we show the colloidal positions just above depinning for $f_d/f_c = 1.1$, where f_c is the critical depinning force, for the same system in Fig. 1(b). Here the colloidal positions are much more disordered, and a portion of the colloids are pinned while the other portion is moving. As f_d is further increased, all the colloids depin and form a moving partially ordered state where the colloids regain a considerable amount of triangular ordering, as seen in Fig. 1(d). The colloid lattice also realigns in the direction of the drive.

The different flow regimes can be identified by the amount of disorder in the lattice and the characteristics of the colloid velocity vs external force curves. In

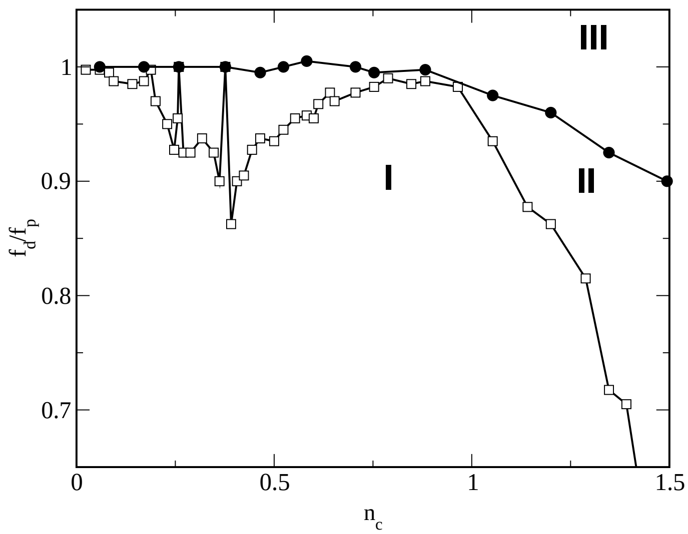

FIG. 3. Flow regions I (pinned), II (plastic), and III (partially ordered) for f_d/f_p vs colloid density n_c at constant $f_p = 2.0$. Open squares: depinning threshold. Filled circles: reordering crossover.

Fig. 2(a) we plot the average colloid velocity V_y and in Fig. 2(b) we show the corresponding fraction of 6-fold coordinated particles P_6 vs the external drive f_d/f_p for the system with $n_c = 1.35$. For a triangular lattice, $P_6 = 1.0$. In Fig. 2(a), there are three regions of the velocity force curve labeled I, II and III. Region I is a pinned state for $f_d/f_p < 0.75$. The plastic flow region II occurs for $0.75 < f_d/f_p < 0.95$ and begins when V_y jumps above zero. In the plastic flow regime, V_y is smaller than it would be if all the colloids were moving, and lies below the value that would be obtained by a linear extrapolation of the velocity-force slope at higher drives. For $f_d/f_p > 0.94$, there is a final jump in V_y indicating that more colloids are now moving, and the system enters region III where V_y increases linearly with f_d and all the colloids move with a uniform velocity. The three regions can also be distinguished in P_6. In the pinned region I where colloids are smectically ordered, there are a significant number of dislocations giving $P_6 = 0.65$. In region II flow, a number of the pinned dislocations annihilate; thus, the average coordination number increases to $P_6 = 0.78$. In region III, the colloids form a mostly triangular lattice, giving $P_6 = 0.95$. In the inset of Fig. 2(a) we show the velocity force characteristics for a system with $n_c = 0.375$ where the lattice makes a transition directly from a pinned triangular lattice to a moving triangular lattice. Here the intermediate jumplike features in V_y are missing due to the absence of a plastic flow regime.

In Fig. 3 we map regions I through III as a function of f_d/f_p vs n_c for fixed $f_p = 2.0$ and fixed d. The depinning threshold shows several peaks and a prominent broad maximum between $0.75 < n_c < 1.0$, corresponding to a triangular colloidal lattice. The peaks occur at

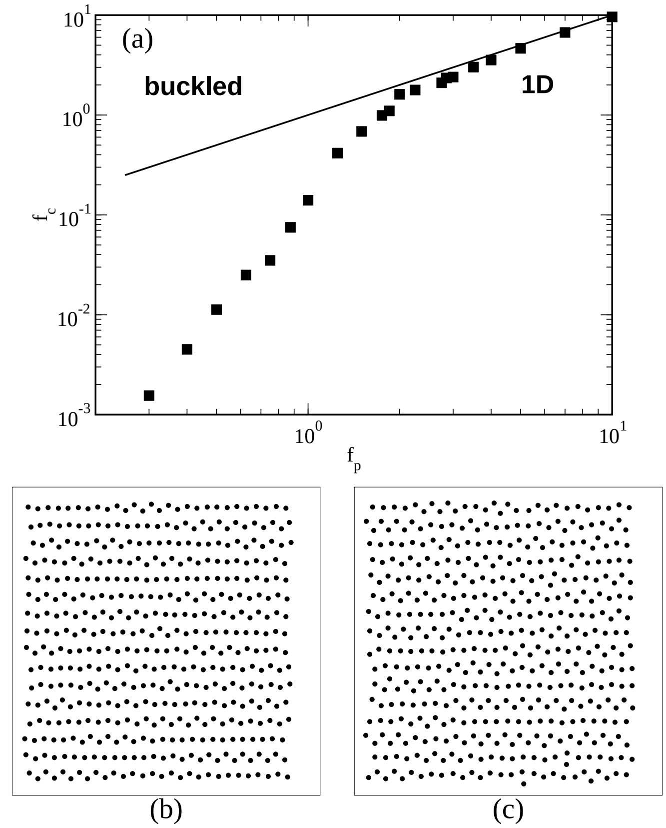

FIG. 4. (a) Squares: critical depinning force f_c vs f_p for fixed $n_c = 1.35$. Solid line: $f_c = f_p$ curve. (b) Buckled state at $f_p = 1.0$ and zero drive. (c) Buckled state at $f_p = 0.75$ and zero drive.

commensurate densities $n_c = 0.38, 0.26$ and 0.185, corresponding to a colloidal lattice constant of $a = \sqrt{2}d$, $\sqrt{3}d$,and $2d$, respectively. At these densities there are no dislocations present in the system and the colloids pass directly from a pinned triangular solid to a moving triangular lattice as a function of driving force without an intermediate disordered flow regime. Region II persists in a small sliver between regions I and III near the commensurability at $n_c = 1$ due to the fact that the system was not perfectly commensurate and there were a small number of dislocations present. There is a broad minimum in the depinning threshold centered around $n_c = 0.45$. Over this range of density there are significant numbers of dislocations present in the system. For $n_c > 1.0$ the depinning threshold drops dramatically with density as dislocations proliferate and the system enters a pinned smectic state. For all densities, once the drive is large enough for all the colloids to depin, the system enters the partially ordered flow regime III. The region III boundary roughly coincides with $f_d = f_p$, although for $n_c > 1.0$, the onset of region III shifts slightly down in drive for increasing n_c due to the enhanced colloidal interactions at these higher densities.

The appearance of the three dynamic regimes is similar

to what is seen for vortices driven over 2D random disorder [19]. In the vortex case, the plastic flow regime occurs when some vortices are trapped in pinning sites while additional interstitial vortices move between the pins. For strong driving, the vortices form a moving smectic state aligned with the drive, due to the effective transverse pinning which is present even at high drives. In the 1D periodic pinning case considered here, the partially ordered regime at high drives is a polycrystalline moving solid rather than a smectic solid since there is no transverse pinning.

In experiments with 1D periodic arrays, it is very straightforward to control the substrate strength by varying the laser intensity. Thus we consider the effects of altering the substrate force f_p, and find that when the substrate is weakened for $n_c > 1.0$, a crossover occurs from the 1D pinned smectic state illustrated in Fig. 1(a) to a buckled configuration. In Fig. 4(a) we plot the critical depinning force f_c vs f_p for a system with fixed $n_c = 1.35$. The straight line in Fig. 4(a) indicates $f_c = f_p$. For $f_p > 1.9$ the pinned state is a one-dimensional smectic structure. As f_p is further increased, f_c increases linearly with f_p and the same pinned smectic state forms. For $f_p \leq 1.9$, patches of the pinned smectic undergo a buckling transition where the colloids along a single row splay out in a staggered manner, as illustrated in Fig. 4(b) for $f_p = 1.0$. Here portions of the lattice remain in the 1D state and coexist with the buckled state. In general the buckled portions do not form adjacent to one another due to the increased inter-row colloidal repulsion that occurs when the buckled state forms. The buckling appears at locations of enhanced stress, where dislocations in the pattern would be present in the 1D pinned case. As f_p is further decreased the buckled areas grow, as seen in Fig. 4(c) for $f_p = 0.75$. The onset of the buckled state coincides with a change from the linear behavior of f_c with f_p to the much more rapid nonlinear decrease for $f_p < 1.9$. The buckled structure is much more weakly pinned than the 1D state since the force acting to push a colloid over the substrate barrier has an additional contribution from the staggered colloids on either side. For pinning forces at which a buckled pinned state forms, there is both a plastic flow regime and a crossover to region III flow as f_d approaches f_p.

In conclusion, we have numerically studied the dynamics and pinning of colloids driven over one-dimensional periodic substrates. We find three general regimes, pinned, disordered, and partially ordered, which can be characterized by the amount of disorder in the colloidal lattice and by features in the velocity force curves. We map these regimes as a function of colloid density and show that peaks in the depinning threshold occur at commensurate densities where triangular or mostly triangular colloid lattices form. As the colloidal density increases for strong substrate strengths, the colloids form a pinned smectic state which transforms to a buckled structure as the substrate strength is reduced. In the pinned smectic state, the depinning threshold decreases linearly with decreasing substrate strength, while in the buckled state, the depinning threshold decreases much faster than linearly with substrate strength.

We thank C. Bechinger and M.B. Hastings for useful discussions. This work was supported by the U.S. DoE under Contract No. W-7405-ENG-36.

[1] C.A. Murray, W.O. Sprenger, and R.A. Wenk, Phys. Rev. B **42**, 688 (1990); K. Zahn, R. Lenke, and G. Maret, Phys. Rev. Lett. **82**, 2721 (1999).
[2] A. Chowdhury, B.J. Ackerson, and N.A. Clark, Phys. Rev. Lett. **55**, 833 (1985).
[3] J. Chakrabarti, H.R. Krishnamurthy, and A.K. Sood, Phys. Rev. Lett. **73**, 2923 (1994).
[4] J. Chakrabarti, H.R. Krishnamurthy, A.K. Sood, and S. Sengupta, Phys. Rev. Lett. **75**, 2232 (1995).
[5] Q.-H. Wei, C. Bechinger, D. Rudhardt, and P. Leiderer, Phys. Rev. Lett. **81**, 2606 (1998); C. Bechinger, M. Brunner, and P. Leiderer, Phys. Rev. Lett. **86**, 930 (2001).
[6] W. Strepp, S. Sengupta, and P. Nielaba, Phys. Rev. E **66**, 056109 (2002).
[7] E. Frey, D.R. Nelson, and L. Radzihovsky, Phys. Rev. Lett. **83**, 2977 (1999).
[8] L. Radzihovsky, E. Frey, and D.R. Nelson, Phys. Rev. E **63**, 031503 (2001).
[9] J. Baumgartl, M. Brunner, and C. Bechinger, Phys. Rev. Lett., in press.
[10] C. Reichhardt and C.J. Olson, Phys. Rev. Lett. **88**, 248301 (2002).
[11] M. Brunner and C. Bechinger, Phys. Rev. Lett. **88**, 248302 (2002).
[12] K. Mangold, P. Leiderer, and C. Bechinger, Phys. Rev. Lett. **90**, 158302 (2003).
[13] R. Agra, F. van Wijland, and E. Trizac, Phys. Rev. Lett. **93**, 18304 (2004).
[14] P.T. Korda, M.B. Taylor, and D.G. Grier, Phys. Rev. Lett. **89**, 128301 (2002).
[15] M.P. MacDonald, G.C. Spalding, and K. Dholakia, Nature **426**, 421 (2003).
[16] A. Gopinathan and D.G. Grier, Phys. Rev. Lett. **92**, 130602 (2004).
[17] M. Baert, V.V. Metlushko, R. Jonckheere, V.V. Moshchalkov, and Y. Bruynseraede, Phys. Rev. Lett. **74**, 3269 (1995); A.N. Grigorenko *et al.*, Phys. Rev. Lett. **90**, 237001 (2003).
[18] B.N.J. Persson, *Sliding Friction: Physical Principles and Applications* (Springer, Heidelberg, 2000), 2nd ed.
[19] L. Balents, M.C. Marchetti and L. Radzihovsky, Phys. Rev. Lett. **78**, 751 (1997); Phys. Rev B **57**, 7705 (1998); P. Le Doussal and T. Giamarchi, Phys. Rev. B **57**, 11356 (1998).